JOURNAL OF BIOMEDICAL OPTICS 2(2), 235–242 (APRIL 1997)

SCATTERING AND BEAM PROFILE MEASUREMENTS OF PLASTIC, SILICA, AND METAL RADIATION WAVEGUIDES

Nathan I. Croitoru, Alexandra Inberg, Reuben Dahan, and Moshe Ben David
Tel-Aviv University, Faculty of Engineering, Dept. Physical Electronics, Tel-Aviv 69978, Israel
(Paper JBO-103 received July 8, 1996; revised manuscript received Feb. 22, 1997; accepted for publication Feb. 26, 1997.)

ABSTRACT

Hollow waveguides (WG) made of plastic, silica, and metals have been developed for mid-IR spectrum transmission and are already being used, mainly in medical applications, in laser surgery and treatments. Characterization of these fibers is one of the important steps that enables further understanding of newly developed methods of preparation or applications. Scattering and beam profile measurements are discussed which have provided new data that may be used for future improvement or applications of these types of waveguides. Data on the roughness of the tube walls of WGs were obtained from backscattering measurements before and after deposition of the guiding layers. This is important for developing WGs for the shorter wavelengths in the mid-IR range (e.g., Er:YAG lasers, $\lambda = 2.94$ nm). Measurements under various bending radii have made it possible to calculate the contribution of scattering as well as absorption and changes in modes of propagation. Beam profile measurements have supplied data on the contribution of coupling to the mode of propagation, and the dependence of delivered energy to a target at a distance on the coupled value of energy. The conditions under which a whisper gallery mode of propagation appears as a function of the radius of bending and the angle of incidence to the normal of the inner wall, were found. *© 1997 Society of Photo-Optical Instrumentation Engineers.* [S1083-3668(97)01102-7]

Keywords infrared radiation, delivery systems, waveguides.

1 INTRODUCTION

In the past few years the applications of infrared laser radiation in medicine have increased drastically and new applications in surgery and treatments using new types of solid-state lasers (e.g., Er:YAG, wavelength $\lambda = 2.94$ μm) were developed. An important limitation of the use of the lasers and other sources of infrared radiation in the wavelength interval of $2.5 < \lambda < 12$ μm arose, since in this region of λ a reliable delivery system similar to that of the core-clad optical fiber or a waveguide suitable for these wavelengths had not been developed. Intensive investigation was carried out and within 3 to 5 years, the characteristics of waveguides for this region of infrared radiation were improved. This has provided a real possibility of developing a delivery system that can be used in biomedical and other applications.

The basic developments in this direction were: (1) The discovery of a new technology for depositing guiding layers (Ag/AgI),[1–3] which enabled the use of any tube with suitable properties (e.g., high flexibility, nontoxic) to make waveguides for medical applications. (2) The reduction of attenuation losses to less than 1 dB/m.[4–6] At present waveguides made of tubes of plastic, quartz glass, sapphire, and metals are already in various stages of being developed.[7–11] The plastic waveguides were the first used in surgery and treatment[12–15] of human patients, which has encouraged further investigation of their development and application in medicine.

One of the important problems that appeared during a study of the possibility of extending the low loss attenuation ($A < 0.5$ dB/m) of all types of waveguides (plastic, glass, and metal) to wavelengths shorter than that of CO_2 (e.g., Er:YAG for hard tissue surgery or visible He:Ne pilot lasers needed in medical applications), was the limitation caused by scattering. Information about the sources of scattering, such as wall roughness and granulations of the deposited Ag/AgI guiding lasers, is not easy to obtain since it is difficult to measure the scattered radiation inside the tube without damaging the tube. The scattered radiation is caused by the multiple reflections on the internal wall of the tube and changes in the distribution of propagated modes along the waveguide.

Earlier papers reported our preliminary studies of this scattering and a possible connection with attenuation.[16–20] In this paper we present the results of studies of the scattering and beam profile of propagated modes of radiation as a function of type

Address all correspondence to Nathan Croitoru. E-mail: croitoru@eng.tau.ac.il

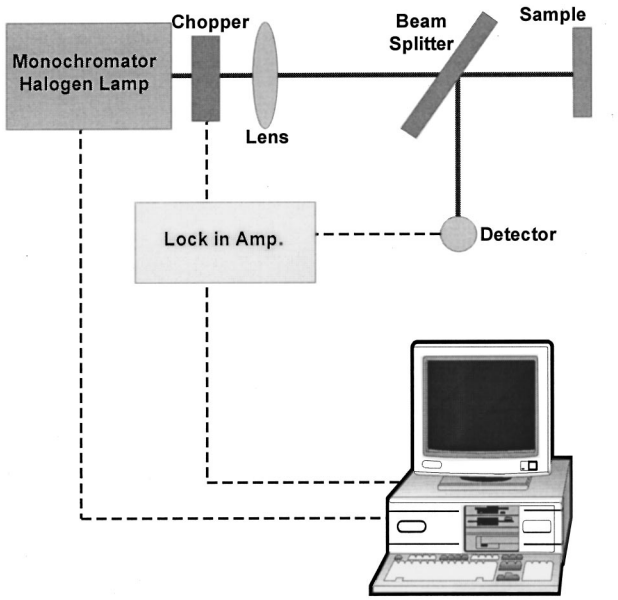

Fig. 1 The experimental setup for scattering measurements.

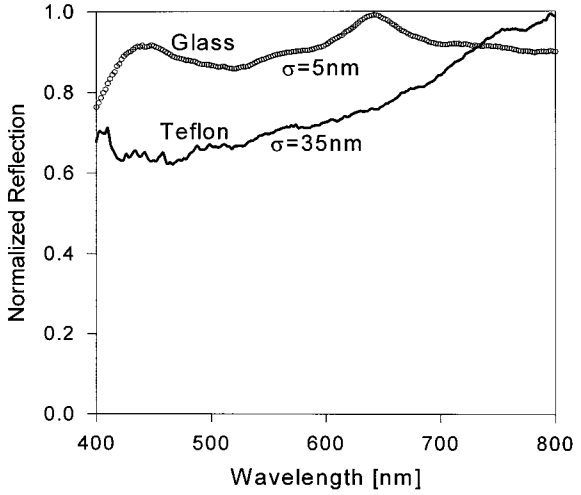

Fig. 2 Normalized reflection intensities of silver on fused silica glass and plastic pieces of tube.

of tube (plastic, glass, and metal), internal diameter (id), length, radius of bending, coupled power or energy, and the conditions for formation of a whispering mode. It will be shown that the experimental results of this study have practical application for mode selection, reduction of scattering losses, and measurements of location of the defects produced in the preparation of the waveguides.

2 EXPERIMENTAL

Samples of Teflon and silica were prepared using the method developed in our laboratory and published earlier.[1,2] The scattering experiments were made using three methods: (1) total integrated scattering (TIS), (2) backscattering reflection (BR), and (3) a nondestructive method (ND). The TIS method was described in Ref. 19 and was used to measure the integral scattering in pieces of waveguide tubes before and after deposition of the guiding metal and dielectric layers. The BR method (Figure 1) was used to measure samples of Teflon or silica glass longitudinally cut into two parts. This allowed us to measure the backscattered reflection from the inner surface of the tube before and after deposition of the Ag and AgI layers. The ND method[18] was used to measure the location of defects on the inner surface of tube before and after deposition of the Ag and AgI layers without cutting the waveguide longitudinally. The light sources for the scattering experiments were a monochromator that has delivered wavelengths of $400 \leqslant \lambda \leqslant 800$ nm and He:Ne ($\lambda = 633$ nm), Ar ($\lambda = 488$ nm), and CO_2 ($\lambda = 10.6$ μm) lasers. A Spiricon beam profiler (LBA-110) system was used for low-power delivery (~ 5 watts) and the Perspex cubes method[10] was used for high-power delivery of the radiation from the waveguides. The Perspex cubes method used high-transparency $2 \times 2 \times 2$ cm^3 cubes of polymethyl methacrylate. Pulses of 2.5 J/s during 0.2 s of laser radiation were applied to the cubes. This changed the viscosity of the material enough that with the pulses applied and rapid cooling, a crater was formed that reproduced the shape of the applied beam. An image of the beam shape was obtained by using a microscope and CCD camera.

3 RESULTS AND DISCUSSION

Theoretical calculation of the scattering produced by defects and granulation of a solid surface in the cylindrical waveguide is not simple because of the very large number and closely located centers of scattering and cylindrical geometry. We took into account that in our cylindrical waveguide, radiation is propagated by multiple reflections from the metal/dielectric layers deposited on the inner part of tube wall. The roughness rms parameter of scattering (σ) for every reflection on the surface is given by Bennett[21]:

$$R(\theta) = R_0 \exp\left\{ -\frac{(4\pi\sigma \cos \theta)}{\lambda} \right\}, \qquad (1)$$

where $R(\theta)$ is the value of reflection as a function of the angle of incidence (θ) to the normal of the wall, λ is the working wavelength, and R_0 is the value of reflection for $\sigma/\lambda = 0$.

For a constant value of θ, the value of R is a function of λ and the roughness parameter (σ). This allows us to obtain the value of σ by taking a constant angle of incidence (e.g., $\theta = 0$) and measuring R as a function of wavelength (λ). Figure 1 shows the setup for this type of measurement of rms (σ) of scattering. Figure 2 shows the dependence of the reflection R/R_0 as a function of λ for Teflon and quartz glass pieces of WG tubes cut longitudinally.

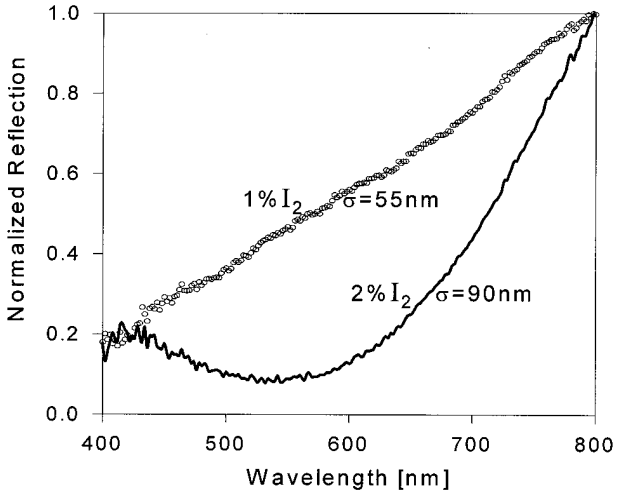

Fig. 3 Normalized reflection intensities of two Ag/AgI layers on fused silica glass pieces of tube.

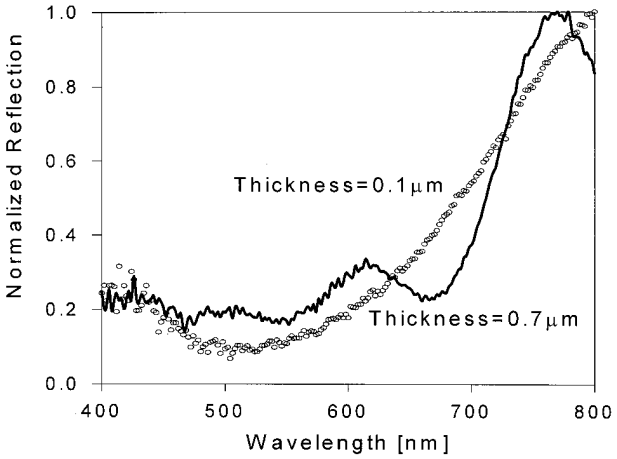

Fig. 4 Normalized reflection intensities of Ag/AgI layers on a fused silica glass tube for $\sigma = 90$ nm.

The scattering in the tubes was measured using the method given in Ref. 18 and total integrated scattering.[19] It can be seen that the quartz glass has a much smaller σ (5 nm) than the Teflon waveguide (35 nm). This is mainly because a very smooth surface of the inner wall of the quartz tube is much easier to fabricate than that of a Teflon tube. Information on the optimum process of chemical deposition of the AgI dielectric layer was obtained by measuring the roughness with this method.

Figure 3 is shows the variation of R/R_0 as a function of λ and the values of σ for two AgI layers deposited from a solution containing 1 and 2% I_2. A comparison of the two graphs in Figure 3 showed that the AgI layer obtained from the solution with the lower concentration of I_2 has a smaller roughness ($\sigma = 55$ nm) than that deposited at the larger concentration of I_2 ($\sigma = 90$ nm). The relative reflection R/R_0 is larger for the film deposited at a low concentration of I_2 than for a deposit at a high concentration of I_2, but only for values of $420 < \lambda < 800$ nm. This is due to the negligible scattering for wavelengths longer than $\lambda > 800$ nm and the negligible reflection (high transmission) in UV ($\lambda < 400$ nm).

A very important result was obtained by comparing the scattering for AgI films of different thicknesses. Figure 4 shows R/R_0 as a function of wavelength for two AgI/Ag films 0.1 and 0.7 μm thick on a plastic WG. Here two concurrent factors affect the R/R_0 ratio: the optical interference due to the thickness of the AgI layer and the scattering. For wavelengths $450\text{ nm} \leqslant \lambda \leqslant 650$ nm, the influence of interference is important. As may be seen, the film that is 0.7 μm thick has an R/R_0 ratio larger than the film that is 0.1 μm. In the region of $650\text{ nm} < \lambda < 750$ nm, the value of the R/R_0 ratio becomes smaller for a 0.7 μm thickness than for the 0.1 μm film. With a further increase in wavelength, the value of R/R_0 is again reversed and becomes larger for 0.7 μm than for a 0.1 μm film. This corresponds to the typical periodic change in intensity of reflected light due to interference. These types of measurements provided important information about the optimum thickness and maximum roughness for a guide that has to deliver a given laser wavelength, or an interval of transmitted λ for radiometry, arrays of lasers, or λ-tuned lasers.

Another important parameter that has to be studied is the dependence of attenuation under bent trajectories in the WG. Bending increases the losses caused by increases in $\cos\theta$[22] and σ because there is an increased probability of larger angles of incidence of rays with scattering centers. Measurements of transmission as a function of wavelength for $400 \leqslant \lambda \leqslant 800$ nm were made for straight and bent WGs.[18] The normalized transmission as a func-

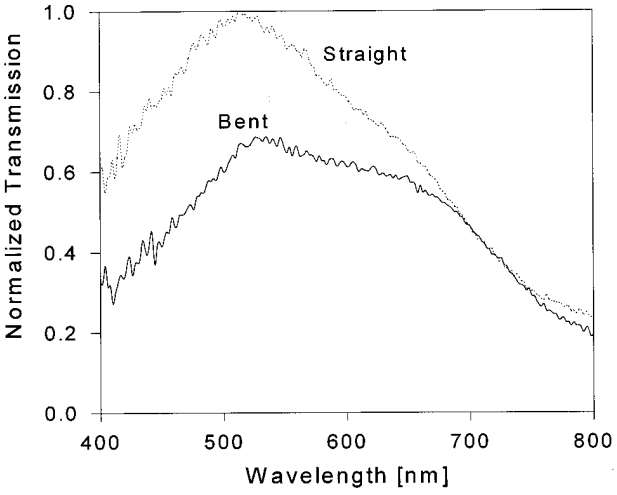

Fig. 5 Normalized transmission intensities of straight (i.d. = 1.0 mm, length=1.0 m) and bent (radius of bending $R = 10$ cm and $\sigma = 25$ nm) plastic waveguides.

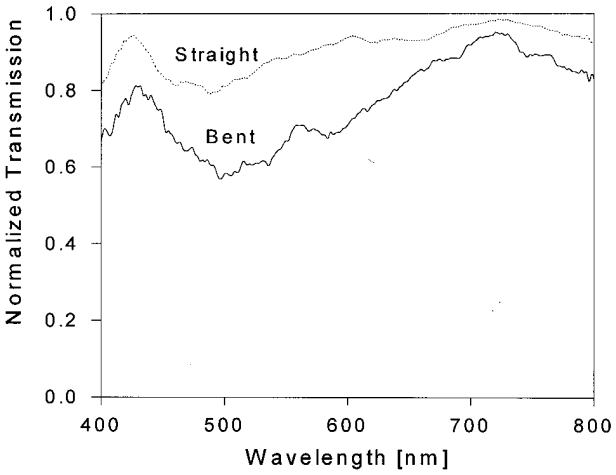

Fig. 6 Normalized transmission intensities of straight and bent (radius of bending $R=10$ cm and $\sigma=20$ nm) glass waveguides.

tion of wavelength for a straight and bent (at a bending radius of $R=10$ cm) plastic waveguide is shown in Figure 5. As can be seen, at shorter wavelengths ($\lambda \leqslant 700$ nm) the bending strongly reduces transmission and for longer wavelengths ($\lambda > 700$ nm), the straight and bent WGs have practically the same transmission. Since scattering is a strong function of $1/\lambda$ [Eq. (1)], it can be assumed that the increase of scattering is dominant in this case for $\lambda \leqslant 700$ nm. The corresponding increase in rms in comparison with that of the straight WG was calculated as $\Delta\sigma=25$ nm.

A similar measurement was made for a silica tube WG where the roughness of the inner wall σ is much smaller than that of the plastic. In this case a λ-dependent transmission after bending is seen only between $500<\lambda<700$ nm since in the interval $400<\lambda<500$ there is maximum of interference (Figure 6). Calculation of increased scattering as a contribution to reduction of transmission has given $\Delta\sigma=20$ nm. This shows that the silica WGs have smaller losses, not only as straight tubes, but also under bending.

Another important factor that has to be studied is the mode of propagation through the WGs. This is because the ratio between the cross section of the bore of the WG is much larger than that of the coupled IR wavelength of the transmitted energy. This makes the type of propagation multimodal, which may have consequences for the attenuation and bending losses that are important in practical applications in medicine or other fields. In medicine a beam is needed at the output from the WG that has a shape similar to that delivered by the laser (which is usually a Gaussian shape). To obtain data on mode propagation, beam profile measurements at energies $E \geqslant 5$ mJ were made employing $2\times2\times2$ cm^3 Perspex cubes. The radiation beam at the output from the WG was directed onto one of the faces of the cube. The radiation melted the Perspex and rapid cooling allowed us to obtain the image of the profile of the incident beam (energy as a function of x, y, and z).

Figure 7 shows, for calibration purposes, a beam profile of a CO_2 laser obtained by a Spiricon beam profiler and by the Perspex cube method. The two images are practically the same. The first measurements were made on straight WGs made of plastic and silica to obtain data on the contribution of wall roughness to the mode of propagation. Figures 8(a), 8(b), and 8(c) show the maximum depth of the crater made by energy delivered to a plastic WG of i.d.=1.0 mm and silica WGs of i.d.=0.5 and 0.7 mm, respectively. As can be seen in Figure 8, the type of

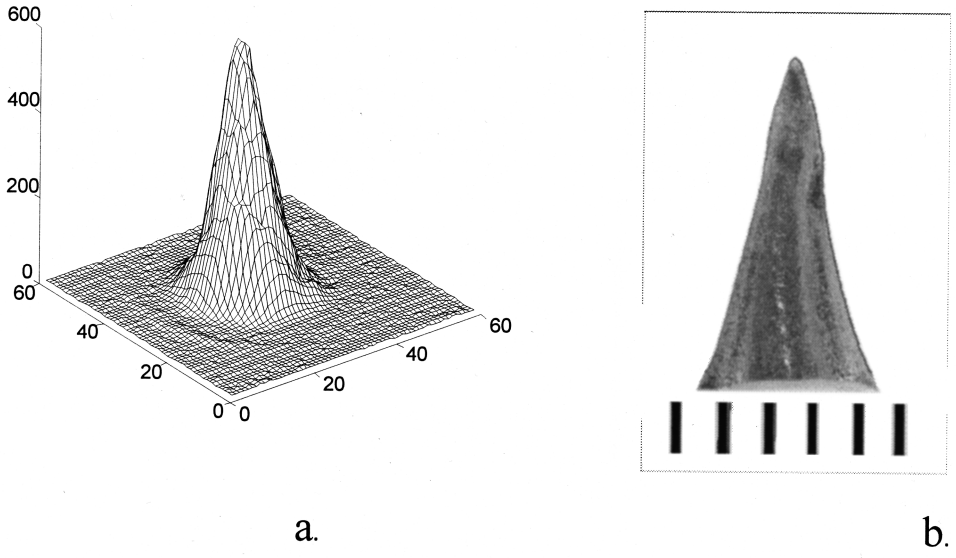

Fig. 7 Comparison between shape of beam measured with (a) Spiricon (60 on the scale equals to 12 mm) and (b) Perspex cube method (distance between bars, 0.5 mm).

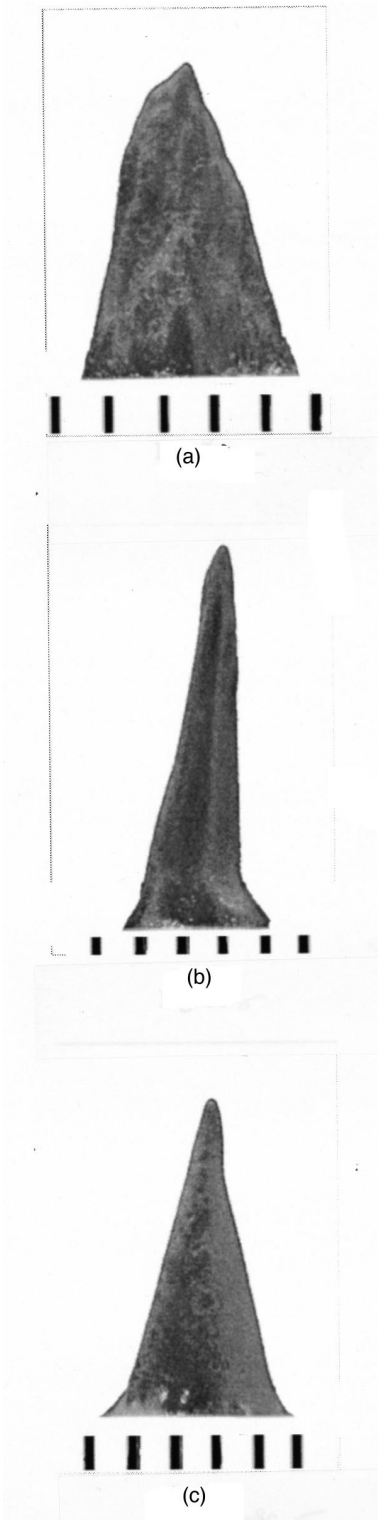

Fig. 8 The crater shape (beam profile) produced by CO_2 laser radiation delivered through a straight waveguide (length=75 cm) of: (a) plastic (i.d.=1.0 mm), (b) fused silica (i.d.=0.5 mm), and (c) fused silica (i.d.=0.7 mm). Distance between bars, 0.5 mm.

material and the size of the inside diameter have an important influence on the shape of the beam profile. The WGs with less wall roughness (silica) and smaller i.d.s (0.5 mm) give the best shape.

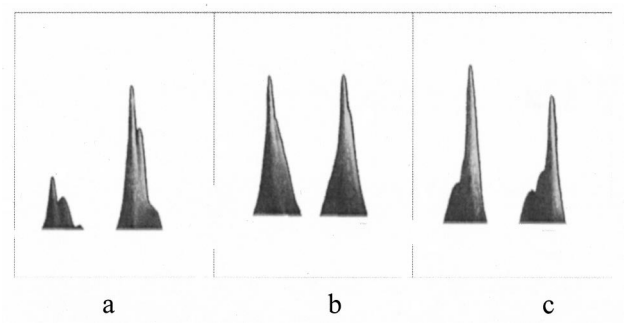

Fig. 9 Influence of eccentric coupling on the shape of a beam delivered by a fused silica waveguide (i.d.=0.7 mm, length =65 cm). (a) Coupling was made to the left side of the bore, (b) coupling was made to the center of the bore, and (c) coupling was made to the right side of the bore. Scanning was made along the inside diameter of the waveguide using 0.1-mm steps.

We have observed that the shape of the propagation mode is sensitive to the coupling. Only if we couple the center of the laser beam exactly to the center of the bore of a hollow WG can we obtain a symmetric image. As can be seen from Figures 9(a), 9(b), and 9(c), shape of the beam remains practically the same (Gaussian) as that delivered by the laser, but nonsymmetric deviations appear for the small (i.d.=0.5) silica WGs because of the difficulties of exact coupling. A clear illustration of the influence of coupling is demonstrated in Figures 9(a), 9(b), and 9(c), which show the profile of a beam from a silica WG of i.d.=0.7 mm. In Figure 9(a), the WG was coupled to the laser beam near to the left end from the center of the wall. The part of the beam nearer to the wall shows no modes, unlike the further end, where the modes can be seen clearly. In Figure 9(b), the coupling to the WG was made near the center. In this case a near-symmetric shape appears. In Figure 9(c) the coupling was made near the right end from the center. Again, the part of the beam nearer to the wall has no modes, unlike the part further from the wall, where the modes appear. This shows that the losses due to scattering and/or absorption by interaction with the wall of the waveguide reduce the higher modes, maintaining only the lower modes, which have the larger energy.

The measurements of beam profile have enabled us also to obtain information on the losses by propagation in free space after the output from the waveguide. Figure 10 shows the dependence of the depth of the main crater in the Perspex (l) as a function of the distance (D) from the tip of the WG to the Perspex cube. With increasing D, the depth l decreases. The larger coupled energy (4 J) delivered to the WG gives larger energy at the output but decreases more rapidly than the smaller energy (2 J)

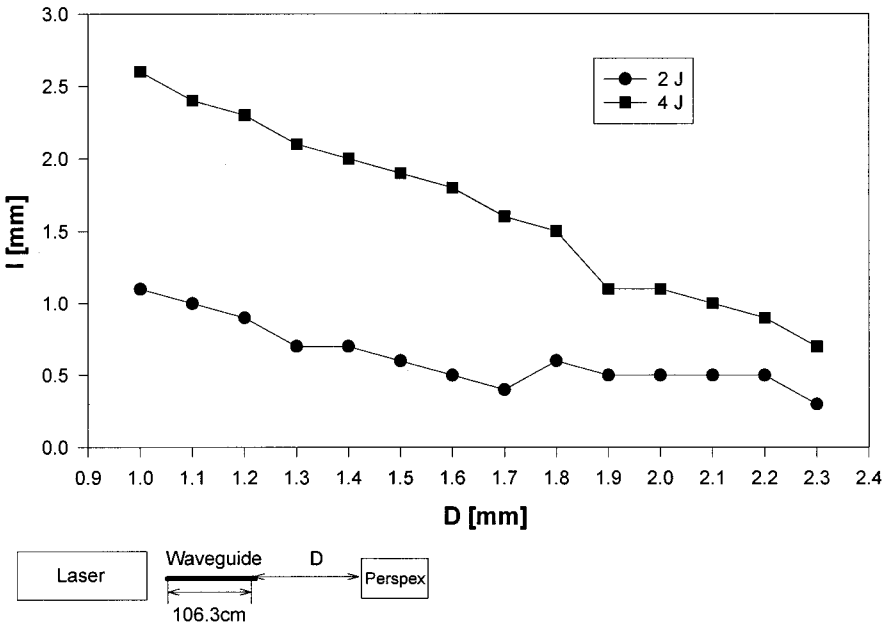

Fig. 10 Maximum crater depth (intensity of radiation) (l) produced by a CO_2 laser versus distance (D) between the tip of the waveguide and the Perspex cube.

with increasing D, tending to be equal for >2.4 mm. The optimum distance at which the beam has to be delivered for practical applications to avoid heating the WG is ($\leqslant 1$ mm); to obtain enough sensitivity to changes in the energy of the delivered beam, it is ~ 1.5 mm.

We also measured the beam profile of the WGs after bending at different radii of curvature R. The results of these measurements are seen in Figure 11.

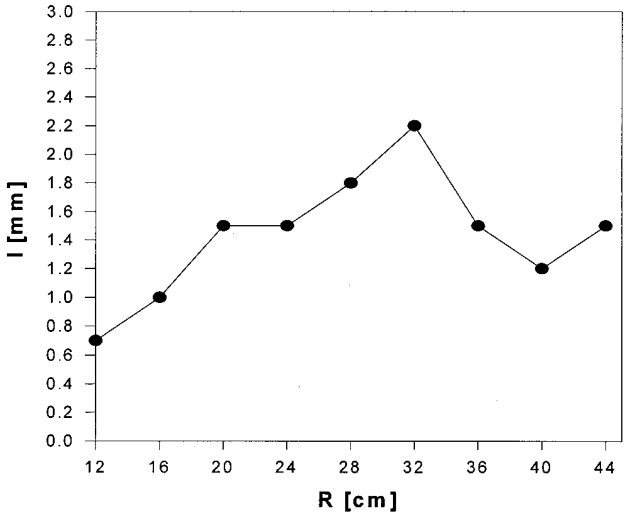

Fig. 11 Maximum crater depth (intensity of radiation) (l) produced in the Perspex cube versus the radius of curvature (R) of a fused silica waveguide (i.d.=0.5 mm).

An important result was observed for bending at a value $R=32$ cm.

Usually if the radius of curvature is increased (less curvature), the depth l has to increase since the delivered energy in the Perspex cube is larger. This is readily seen for $R<32$ cm. For bending at $R=32$ cm, the length l reaches a maximum (2.2 mm) and with a further increase to $R>32$, it decreases; for $R=40$ cm, the value $l=1.1$ mm (half of that of the maximum $l=2.2$ mm). This suggests, that with a curvature radius of 32 cm, the given conditions of coupling between the laser and the WG, and the cross-section diameter of the WG bore, a total or partial whisper gallery mode of propagation,[23] was obtained in which the energy is concentrated near one part of the inner wall and the losses are decreased.

We calculated the critical conditions for a whisper gallery mode of propagation. Figure 12 shows the incidence of a ray with the inner wall under an angle θ. The radius of curvature is R and the bore radius of the waveguide is d. The condition for whisper gallery propagation is $0\leqslant x\leqslant 2d$, where $x=AC$ (Figure 13), $R>2d$ and $\theta\geqslant 80$ deg.[22,24]

The relation between x, $(R+d)$ and θ is given by:

$$(R+d)(1-\sin\theta)=x. \tag{2}$$

The conditions for a whisper gallery mode of propagation were calculated using Eq. (2) for $d=0.5$ mm and various R and $\sin\theta$. The results are shown in Figure 13. The experimental values obtained for WGs by measuring the maximum deliv-

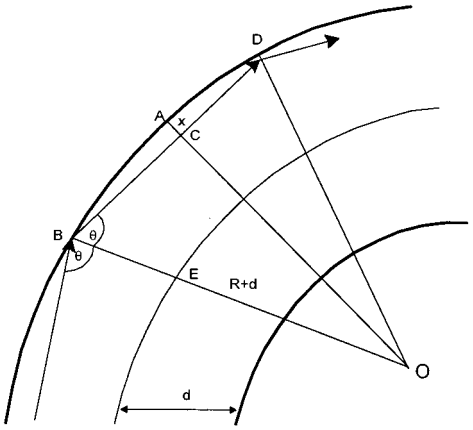

Fig. 12 Geometrical representation of parameters and incidence of a ray to obtain a whisper gallery mode of propagation.

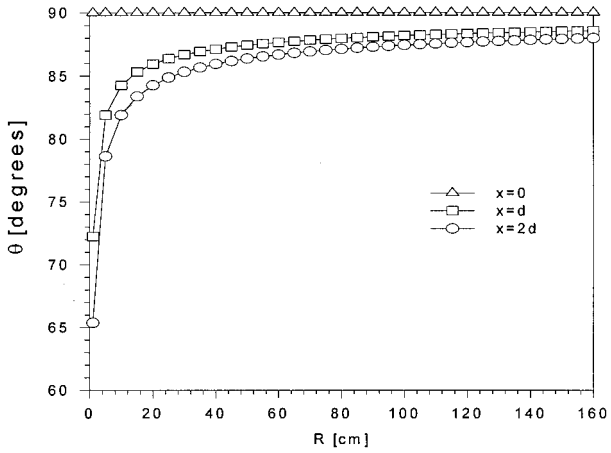

Fig. 13 The angle of incidence for whisper gallery mode propagation (θ) versus radius of curvature (R) of the waveguide (i.d.=0.5 mm). The value $x=AC$ (see Fig. 12).

ered energy at a given R and d using the beam profile method of Perspex cubes may confirm our hypothesis of a whisper gallery and Eq. (2). However, more measurements have to be made and other possible explanations of the appearance of the maximum investigated—for instance, interference between the lower and higher modes.[25]

4 CONCLUSIONS

Scattering measurements on plates and tubes of plastic and silica covered with a silver (Ag) layer and a silver iodine (AgI) overlayer were performed and data about the rms roughness of the tube walls and guiding Ag/AgI layers were obtained.

- The results obtained from scattering measurements were used to develop and improve waveguides in the mid-IR region of the spectrum.
- Measurements of scattering under bending have enabled us to calculate the increase of losses due to increase of scattering ($\Delta\sigma$) and to separate it from other factors, such as absorption in guiding films or angle of incidence with the wall.
- Beam profile measurements for straight WGs using the simple method of Perspex cubes have provided data on the contribution of the type of tube (plastic or silica) and of the inside diameter to the modes of propagation. These data are very important for preparation of WGs and for medical applications.
- Beam profile measurements have shown that the coupling of laser radiation with a WG has to be made in the center of the bore of a hollow waveguide. Deviations of center coupling give nonsymmetrical shapes of the beam delivered from the WG.
- Information was obtained on the decrease of delivered energy from the tip of the WG to a target as a function of distance D and coupled energy from the laser. We show that the optimal distance for minimum divergence is 1.5 mm.
- The conditions under which a whisper gallery mode propagation appears (radius of bending for constant coupling focal length) were determined using the Perspex cube beam profile method.

Our experiments show that scattering and beam profile measurements are methods that enable one to obtain important information on the quality of deposited guiding layers and to predict the conditions of maximum power delivery by a whisper gallery mode of propagation.

REFERENCES

1. N. Croitoru, J. Dror, E. Goldenberg, D. Mendlovic, and I. Gannot, ''Hollow fiber waveguides and method of making them,'' U.S. Patent, 4,930,863 (June 5, 1990).
2. R. Dahan, J. Dror, and N. Croitoru, ''Characterization of chemically formed silver iodide layers for hollow infrared guides,'' *Mat. Res. Bull.* **27**, 761–766 (1992).
3. M. Alaluf, J. Dror, R. Dahan, and N. Croitoru, ''Plastic hollow fibers as a selective infrared radiation transmission medium,'' *J. Appl. Phys.* **72** (9), 3878 (1992).
4. J. A. Harrington, ''Laser power delivery in infrared fiber optics,'' *Proc. SPIE* **1649**, 14–22 (1992).
5. N. Croitoru, J. Dror, and I. Gannot, ''Characterization of hollow fibers for the transmission of infrared,'' *Appl. Opt.* **29**, 1805–1809 (1990).
6. Y. Kato, M. Osawa, and M. Miyagi, ''Transmission characteristics of polyimide-coated silver hollow glass-waveguides for medical applications,'' *Proc. SPIE* **2328**, Biomedical Optoelectronic Devices and Systems II, Europto, 16–21 (1994).
7. J. A. Harrington and Y. Matsuura, ''Review of waveguide technology,'' *Proc. SPIE*, **2396**, Biomedical Optoelectronic Instrumentation, 4–14 (1995).
8. J. Dror, A. Inberg, A. Elboim, R. Dahan, and N. Croitoru, ''New performances and applications of fused silica and

plastic waveguides,'' *Proc. SPIE*, **2396**, Biomedical Optoelectronic and Instrumentation, 106–114 (1995).
9. Y. Kato, M. Osawa, S. Kubota, M. Miyagi, Shin-ichi Abe, M. Aizawa, and S. Onodera, ''Heat-resisting polymer-coated silver hollow glass waveguides for medical applications,'' *Proc. SPIE*, **2396**, Biomedical Optoelectronic and Instrumentation, 101–105 (1994).
10. R. Dahan, J. Dror, A. Inberg, and N. Croitoru, ''Study of physical parameters which influence the quality of hollow waveguides,'' *Proc. SPIE*, **2631**, Medical and Fiber Sensors and Delivery Systems, Europto, 156–160 (1994).
11. J. Dror, A. Inberg, R. Dahan, A. Elboim, and N. Croitoru, ''Influence of heating on performances of flexible hollow waveguides for the mid-infrared,'' *J. Phys. D., Appl. Phys.* **29**, 1–9 (1996).
12. I. Kaplan, S. Giller, J. Dror, I. Gannot, and N. Croitoru, ''Preliminary experiments of possible uses in medicine of novel plastic fibers for transmission of CO_2 radiation,'' *Lasers Surg. Med.* **10**, 291–293 (1990).
13. I. Gannot, J. Dror, S. Calderon, I. Kaplan, and N. Croitoru, ''Flexible waveguides for IR laser radiation and surgery applications,'' *Laser Surg. Med.* **14**, 184–189 (1994).
14. S. Calderon, I. Gannot, G. Gal, and N. Croitoru, ''Utiliation du laser CO_2 a guide d'ondes flexible en chirurgie orale et maxillo-faciale,'' *Realité Cliniques*, **5**, 293–300 (1994).
15. N. Croitoru, ''Hollow waveguides for infrared applications,'' *Trends Lightwave Tech.* **1**, 73–86 (1994).
16. Y. Matsuura, M. Saito, and M. Miyagi, ''Loss characteristics of circular hollow waveguides for incoherent radiation,'' *J. Opt. Soc. Am.* **A6**, 423–427 (1989).
17. R. Dahan, A. Inberg, J. Dror, and N. Croitoru, ''Scattering phenomenon investigation of the guiding surface of infrared waveguides for application in medicine,'' *Proc. SPIE*, **2328**, Biomedical Optoelectronic Devices and Systems II, Europto, 45–51 (1994).
18. R. Dahan, J. Dror, A. Inberg and N. Croitoru, ''Nondestructive method for attenuation measurements in optical hollow waveguides,'' *Opt. Lett.* **20**, 1–2 (1995).
19. R. Dahan, J. Dror, A. Inberg, and N. Croitoru, ''Scattering of IR and visible radiation from hollow waveguides,'' *Proc. SPIE*, **2396**, Biomedical Optoelectronic Instrumentation, 115–119 (1995).
20. M. Miyagi, A. Hongo, A. Aizawa, and S. Kawakami, ''Fabrication of germanium-coated nickel hollow waveguides for infrared transmission,'' *Appl. Phys. Lett.* **43**, 430–432 (1993).
21. J. M. Benett, ''Comparison of techniques for measuring the roughness of optical surfaces,'' *Opt. Eng.* **24** (3), 380–387 (1985).
22. O. Morhaim, D. Mendlovic, I. Gannot, J. Dror, and N. Croitoru, ''Ray model for transmission of infrared radiation through multibent cylindrical waveguides,'' *Opt. Eng.* **30**, 1886–1891 (1991).
23. M. Miyagi, ''Bending losses in hollow and dielectric tube leaky waveguide,'' *Appl. Opt.* **20**, 1221–1229 (1981).
24. J. Dror, A. Inberg, R. Dahan, A. Elboim, and N. Croitoru, ''Influence of heating on performances of flexible hollow waveguides for the mid-infrared,'' *J. Phys. D. Appl. Phys.* **29**, 569–577 (1996).
25. D. Su, S. Somkuamparit, D. R. Hall, and J. D. C. Jones, ''Hollow core waveguides for high quality CO_2 laser beam delivery: exploitation of the induced mode coupling,'' *Opt. Comm.* **114**, 255–261 (1995).